

INTEGRATION OF THE NONDIVERGENT BAROTROPIC VORTICITY EQUATION WITH AN ICOSAHEDRAL-HEXAGONAL GRID FOR THE SPHERE¹

ROBERT SADOURNY,² AKIO ARAKAWA, and YALE MINTZ

Department of Meteorology, University of California, Los Angeles, Calif.

ABSTRACT

A finite difference scheme is developed for numerical integration of the nondivergent barotropic vorticity equation with an icosahedral-hexagonal grid covering the sphere. The grid is made by dividing the 20 triangular faces of an icosahedron into smaller triangles, the vertices of which are the grid points. Each grid point is surrounded by six neighboring points, except the 12 vertices of the icosahedron which are surrounded by five points. The difference scheme for the advection of vorticity exactly conserves total vorticity, total square vorticity, and total kinetic energy. A numerical test is made, with a stationary Neamtan wave as the initial condition, by integrating over 8 days with 1-hr. time steps and a grid of 1002 points for the sphere. There is practically no distortion of the waves over the 8 days, but there is a phase displacement error of about 1° of long. per day toward the west.

1. INTRODUCTION

For numerical integration of the equations of atmospheric motion in the global domain, it is desirable to use a quasi-uniform grid which divides the sphere into elements that are nearly equal in area and in shape.

Gates and Riegel [1] and Kurihara [2] constructed global grids with quasi-uniform mesh size, using the principle of a decreasing number of points along the latitude circles as one approaches the poles.

In our scheme, the sphere is divided into 20 spherical triangles (to form a spherical icosahedron), with each triangular face further subdivided into smaller triangles. This division of the globe was used for geomagnetic studies by Vestine et al. [3]. We desire to use this grid for numerical integration of the equations of atmospheric motion. As a first step in this direction, we are showing here a method for integration of the nondivergent barotropic vorticity equation.³

great circles, but the equalities of the shape and areas of the triangles are not maintained.

In this paper we have chosen a somewhat different procedure, which better preserves the equality of grid distances. We start from a spherical icosahedron, made of 20 equal spherical triangles, one face of which is shown in figure 2. Let ABC be the face of the spherical triangle.

2. DESCRIPTION AND INDEXING OF THE GRID

There are several ways to construct a grid based on the icosahedron. The plane icosahedron inscribed into the sphere has 12 vertices and 20 plane faces which are equilateral triangles of equal size (fig. 1). Each triangular face can be divided into n^2 equal equilateral triangles by drawing $(n-1)$ equally spaced parallels to each side. The grid thus obtained can be projected radially onto the surface of the sphere. All of the projected lines are arcs of

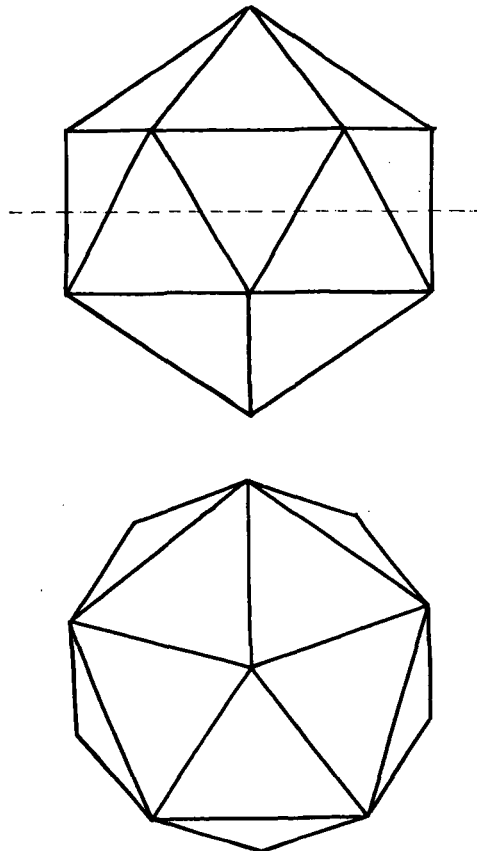


FIGURE 1.—The plane icosahedron.

¹ U.C.L.A. Department of Meteorology, Contribution No. 146.

² Present affiliation: Service d'Aeronomie du C.N.R.S., 91-Verrières-le-Buisson, France.

³ While this manuscript was being prepared for publication, we learned that a similar calculation, with practically the same grid scheme, had been made by Mr. David Williamson, of the Meteorology Department, Massachusetts Institute of Technology, and subsequently issued as NCAR Manuscript No. 443.

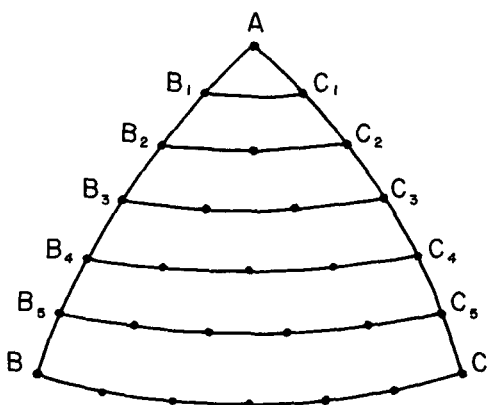


FIGURE 2.—Construction of the grid on a spherical triangle, for $n=6$.

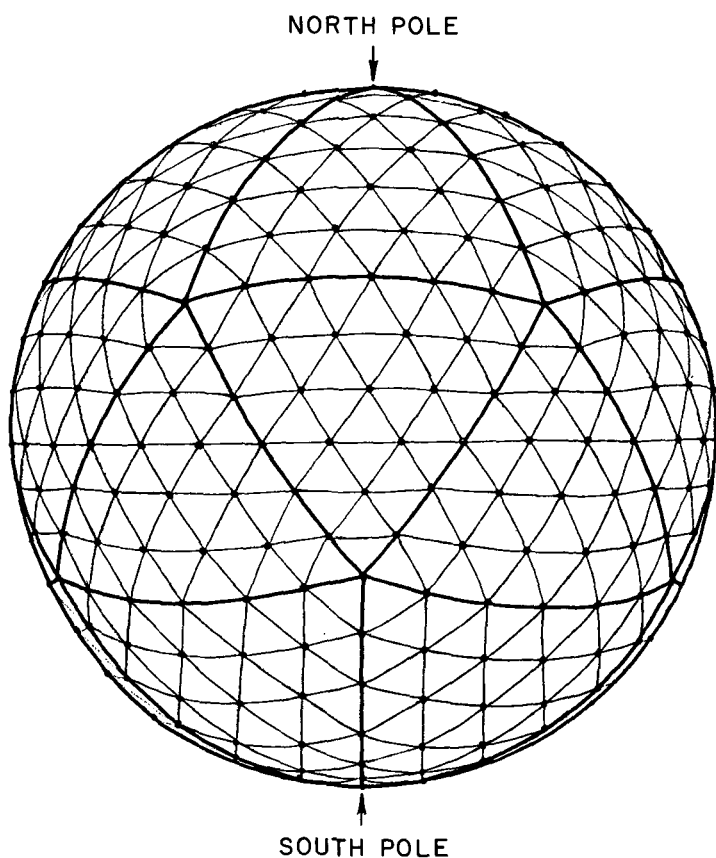


FIGURE 3.—Representation of the icosahedral-hexagonal grid, for $n=6$.

We divide the great circle arcs AB and AC into n equal arcs, to give the points B_1, \dots, B_{n-1}, B_n (coinciding with B) and C_1, \dots, C_{n-1}, C_n (coinciding with C). Then we take each great circle arc B_iC_i and divide it into i equal parts. The distance between adjacent grid points, in any direction, varies by less than 10 percent over the spherical triangle.

If O is the center of the sphere, then we have to solve the linear system

$$\begin{aligned} \vec{OA} \cdot \vec{OB}_i &= \cos\{(i/n)\widehat{AB}\}, \\ \vec{OB} \cdot \vec{OB}_i &= \cos\{(1-i/n)\widehat{AB}\}, \\ \vec{OA} \cdot \vec{OB}_i + \vec{OB} \cdot \vec{OB}_i &= 0. \end{aligned}$$

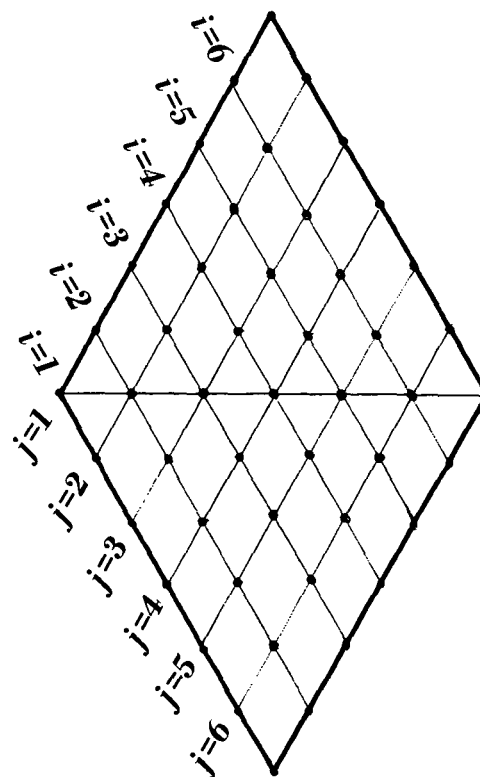


FIGURE 4.—Indexing of a rhombus cell, for $n=6$.

The third equation expresses the condition that O, A, B, B_i be coplanar. Here the radius of the sphere is equal to 1, and \widehat{AB} is the arc AB measured in radians.

In cartesian coordinates this system is expressed by

$$\begin{aligned} x_A x_i + y_A y_i + z_A z_i &= \alpha_A, \\ x_B x_i + y_B y_i + z_B z_i &= \alpha_B, \\ \begin{vmatrix} x_i & y_i & z_i \\ x_A & y_A & z_A \\ x_B & y_B & z_B \end{vmatrix} &= 0, \end{aligned}$$

where $\alpha_A = \cos\{(i/n)\widehat{AB}\}$ and $\alpha_B = \cos\{(1-i/n)\widehat{AB}\}$. We solve this system for x_i, y_i, z_i .

Each point on the face or edge of one of the 20 faces of the icosahedron is now surrounded by six triangles and is therefore in the center of a hexagon. However, the points which form the vertices of the icosahedron are surrounded by only five triangles and therefore these 12 singular points are the centers of pentagons.

As shown in figure 3, the poles were chosen as two pentagonal points. The triangular faces of the icosahedron were arranged into 10 pairs of adjoining faces, forming 10 rhombuses; five around the North Pole and five around the South Pole, indexed from 1 to 10. The grid points inside each rhombus were indexed with two indices (i, j) , as shown in the example of figure 4. The two Poles, where five rhombuses meet, are treated separately, but with the same finite difference scheme as the other vertices.

For the simplicity of the programming, all the fields were defined in a $10 \times (n+2) \times (n+2)$ array. The overlapping simplified the programming on the boundaries

of the rhombuses, the extra values being periodically redefined by identifications.

In our numerical example, we used a coarse grid by taking $n=10$. This gave 1002 grid points for the entire sphere. With $n=10$, the areas of the hexagons fall between 0.481 and $0.551 \times 10^6 \text{ km}^2$. The ratio of minimum to maximum grid area is a function of the resolution and decreases with increasing n .

3. THE FINITE DIFFERENCE JACOBIAN FOR A TRIANGULAR GRID

The nondivergent barotropic vorticity equation can be written

$$\frac{\partial \zeta}{\partial t} = J(\zeta, \psi),$$

where ψ is the stream function, ζ is the vorticity of the horizontal wind, t is time, and J is the Jacobian operator.

Arakawa [4] showed that certain integral constraints which hold for the differential form of the above equation will also be maintained in the finite difference analog of this equation, if the finite difference Jacobian is written in an appropriate way.

The integral constraints which are maintained in this scheme are the kinetic energy, the total vorticity, and the total square vorticity. When these properties are conserved, nonlinear computational instability cannot occur. Moreover, the spectral distribution of the kinetic energy is constrained to maintain its average scale.

The Jacobian in differential form, $J(\zeta, \psi)$, has the following property:

$$\left. \begin{aligned} \iint_D \psi^n J(\zeta, \psi) d\sigma &= \frac{-1}{n+1} \oint_C \psi^{n+1} \frac{\partial \zeta}{\partial s} ds \\ \iint_D \zeta^n J(\zeta, \psi) d\sigma &= \frac{1}{n+1} \oint_C \zeta^{n+1} \frac{\partial \psi}{\partial s} ds \end{aligned} \right\} \quad (1)$$

for $n \neq -1$. Here D is any domain bounded by the curve C , and $\partial/\partial s$ refers to the derivative along the curve C .

If we let the domain, D , be the entire surface of the sphere, S , equation (1) reduces to

$$\left. \begin{aligned} \iint_S \psi^n J(\zeta, \psi) d\sigma &= 0, \\ \iint_S \zeta^n J(\zeta, \psi) d\sigma &= 0. \end{aligned} \right\} \quad (1')$$

In this nondivergent, barotropic fluid, the kinetic energy per unit area is

$$K = \frac{1}{2} \nabla \psi \cdot \nabla \psi.$$

Then

$$\frac{\partial K}{\partial t} = \nabla \psi \cdot \nabla \frac{\partial \psi}{\partial t} = \nabla \cdot \left(\psi \nabla \frac{\partial \psi}{\partial t} \right) - \psi^2 \nabla \cdot \frac{\partial \psi}{\partial t}.$$

Integrating over the whole sphere, the time change of the total kinetic energy is

$$\begin{aligned} \frac{\partial}{\partial t} \iint_S K d\sigma &= - \iint_S \psi \frac{\partial \zeta}{\partial t} d\sigma \\ &= - \iint_S \psi J(\zeta, \psi) d\sigma. \end{aligned}$$

From the above, and by setting $n=1$ in equation (1'), we see that the total kinetic energy is conserved. In a similar way, it can be shown that the conservations of total vorticity and total square vorticity also come from the integral constraints of the differential Jacobian given by equation (1'), for $n=0$ and $n=1$.

In the following, $*$ will refer to a grid point and Δ to a triangle. We start from the quantities ψ_i and ζ_i defined at the vertices of each triangle Δ . By linear interpolation from ψ_i and ζ_i , we can define $\tilde{\psi}$ and $\tilde{\zeta}$ everywhere. These interpolated values, which we call $\tilde{\psi}$ and $\tilde{\zeta}$, are continuous functions of space. Because of the linear interpolation, the gradients $\nabla \tilde{\psi}$ and $\nabla \tilde{\zeta}$ are constant within each individual triangle, but discontinuous at the boundaries. However, the tangential derivatives, $\partial \tilde{\zeta} / \partial s$ and $\partial \tilde{\psi} / \partial s$, are continuous at the boundaries of the triangles.

$J(\tilde{\psi}, \tilde{\zeta})$ is constant inside each triangle and is called J_Δ . It has the properties

$$\left. \begin{aligned} \iint_\Delta \tilde{\psi}^n J_\Delta d\sigma &= \frac{-1}{n+1} \oint_\Gamma \tilde{\psi}^{n+1} \frac{\partial \tilde{\zeta}}{\partial s} ds, \\ \iint_\Delta \tilde{\zeta}^n J_\Delta d\sigma &= \frac{1}{n+1} \oint_\Gamma \tilde{\zeta}^{n+1} \frac{\partial \tilde{\psi}}{\partial s} ds, \end{aligned} \right\} \quad (2)$$

where Γ is the boundary of the triangle Δ .

Summing over all the triangles in S , and owing to the continuity of $\tilde{\psi}$, $\tilde{\zeta}$, $\frac{\partial \tilde{\psi}}{\partial s}$, $\frac{\partial \tilde{\zeta}}{\partial s}$, we get

$$\left. \begin{aligned} \iint_S \tilde{\psi}^n J_\Delta d\sigma &= 0, \\ \iint_S \tilde{\zeta}^n J_\Delta d\sigma &= 0, \end{aligned} \right\} \quad (2')$$

which shows that J_Δ satisfies all of the above integral constraints. J_Δ is also a three point finite difference approximation for the Jacobian. Setting $n=0$ in (2), and rewriting the line integral as a sum, we get

$$J_\Delta = \frac{1}{S_\Delta} \sum_{i=1}^3 \frac{(\zeta_i + \zeta_{i+1})}{2} (\psi_{i+1} - \psi_i), \quad (3)$$

where i is 1, 2, or 3 and $i+1=1$ when $i=3$. S_Δ is the area of the triangle. This formula is valid whatever the shape of the triangle.

For the numerical integration we need a Jacobian, J_* , defined at the grid points which are the vertices of the triangles. Just as J_Δ was obtained by taking the circulation of $(\zeta \nabla \psi)$ along Γ and dividing by S_Δ , so we can similarly obtain J_* by taking the circulation of $(\zeta \nabla \psi)$ along the sides of the polygon, P_* , made up of the six triangles (five at the singular points) which have that point as a common vertex. If $N=5$ or 6 is the number of sides of this polygon, we get

$$J_* = \frac{1}{S_*} \sum_{i=1}^N \frac{(\zeta_i + \zeta_{i+1})}{2} (\psi_{i+1} - \psi_i), \quad (4)$$

where i refers to the vertices of P_* , ordered sequentially counterclockwise (where $N+1$ is replaced by 1) and S_* is the area of the polygon.

S_*J_* is the summation of the circulations, $S_{\Delta}J_{\Delta}$, previously considered for all the triangles Δ surrounding the point.

This expression of the Jacobian can also be written in several equivalent forms:

$$J_* = \frac{1}{S_*} \sum_{i=1}^N \frac{1}{2} \zeta_i (\psi_{i+1} - \psi_{i-1}), \quad (4a)$$

$$J_* = \frac{1}{S_*} \sum_{i=1}^N \frac{1}{2} \psi_i (\zeta_{i-1} - \zeta_{i+1}), \quad (4b)$$

$$J_* = \frac{1}{S_*} \sum_{i=1}^N \frac{1}{2} (\zeta_0 + \zeta_i) (\psi_{i+1} - \psi_{i-1}). \quad (4c)$$

These formulas are valid for either plane or spherical triangles and polygons.

Summing each of these three formulas over the whole globe, we get

$$\sum_S \zeta_0 J_* S_* = 0, \quad (4a')$$

$$\sum_S \psi_0 J_* S_* = 0, \quad (4b')$$

$$\sum_S J_* S_* = 0, \quad (4c')$$

where the subscript 0 refers to the grid point where J_* is computed. These vanishing global sums are approxi-

mations for the integral constraints on the differential Jacobian:

$$\iint_S \zeta J(\zeta, \psi) d\sigma = 0,$$

$$\iint_S \psi J(\zeta, \psi) d\sigma = 0,$$

$$\iint_S J(\zeta, \psi) d\sigma = 0,$$

which lead, respectively, to the conservations of total square vorticity, total kinetic energy, and total vorticity.

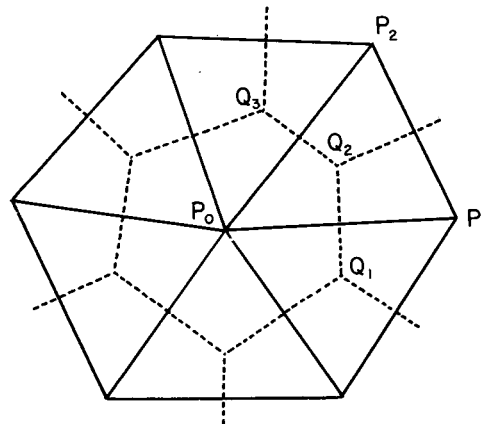


FIGURE 5.—Scheme for the Laplacian operator.

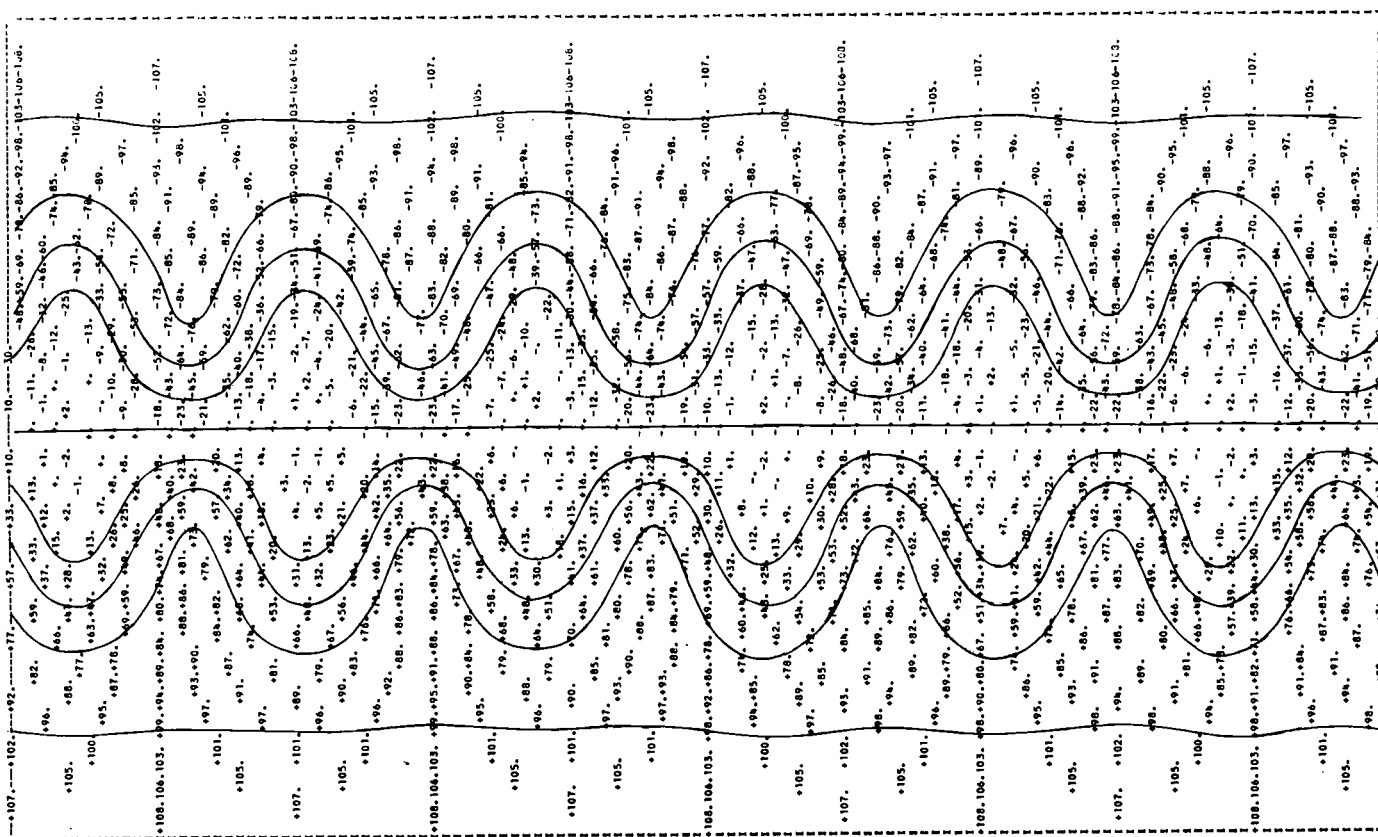


FIGURE 6.—Initial streamfunction (Mercator projection).

4. THE LAPLACIAN L_*

Taking, again, the indices $0, (1, \dots, N)$, we define the point Q_i equidistant from the three vertices P_0, P_1 , and P_{i-1} (the center of the circumscribed circle) such that $Q_i Q_{i+1}$ is the perpendicular bisector of the arc $P_0 P_i$, as shown in figure 5.

Then $\nabla^2 \psi = \nabla \cdot (\nabla \psi)$ is easily computed, at the point P_0 , as the flux of $\nabla \psi$ flowing out of the polygon (Q_i) divided by the area s_* of this polygon, or

$$L_* = \frac{1}{s_*} \sum_{i=1}^N \frac{Q_i Q_{i+1}}{P_0 P_i} (\psi_i - \psi_0).$$

Notice that the sum of all the contiguous nonoverlapping polygons (Q_i) covers the sphere. In the actual computation the extreme values of the ratio $\frac{Q_i Q_{i+1}}{P_0 P_i}$ were found to be 0.33225 and 0.86380.

5. THE NUMERICAL EXPERIMENT

The scheme was tested by integrating over several days of simulated time from an initial state which is a stationary solution of the barotropic vorticity equation,

$$\frac{\partial \zeta}{\partial t} = J(\zeta + f, \psi),$$

$$\zeta = \nabla^2 \psi,$$

where f is the Coriolis parameter.

A stationary solution, given by Neamtan [5], is

$$\psi(\varphi, \lambda) = A \sin m \lambda P_n^m(\sin \varphi) - B R^2 \sin \varphi,$$

$$B = \frac{2\Omega}{n(n+1) - 2},$$

where φ and λ are latitude and longitude, R is the earth's radius, and Ω is the rate of the earth's rotation.

The coefficient A was arbitrarily chosen as 1000 m.²/sec. The wave number $m=6$ was chosen to avoid coincidence with the five-fold periodicity of the grid around the poles. $n=7$ allows a symmetry of the stationary solution about the equatorial plane, whereas the grid pattern has no such symmetry. One-hour time steps were used, together with a second order Adams-Bashforth time differencing scheme, described by Lilly [6]. Forward differencing was used for the first time step.

The results of the test are shown in figures 6 through 9. Comparing figures 6, 7, and 8, we see practically no distortion of the waves over the 8 days of integration. However, within the uncertainty of the interpolation, there is a westward phase displacement error of about 7° of long. in 8 days. This displacement error comes from the large grid distance that was used.

After 8 days, the relative error of the average square vorticity is 5×10^{-4} and the relative error of the average kinetic energy is 3×10^{-3} , as shown in figure 9. These small errors are due to the slight instability of the Adams-Bashforth time differencing scheme for average square vorticity, and to the accumulation of the relaxation residuals for the kinetic energy.

6. CONCLUSION

The conclusion we draw is that this space differencing scheme, for numerical integration of the nondivergent barotropic vorticity equation with the icosahedral-hex-

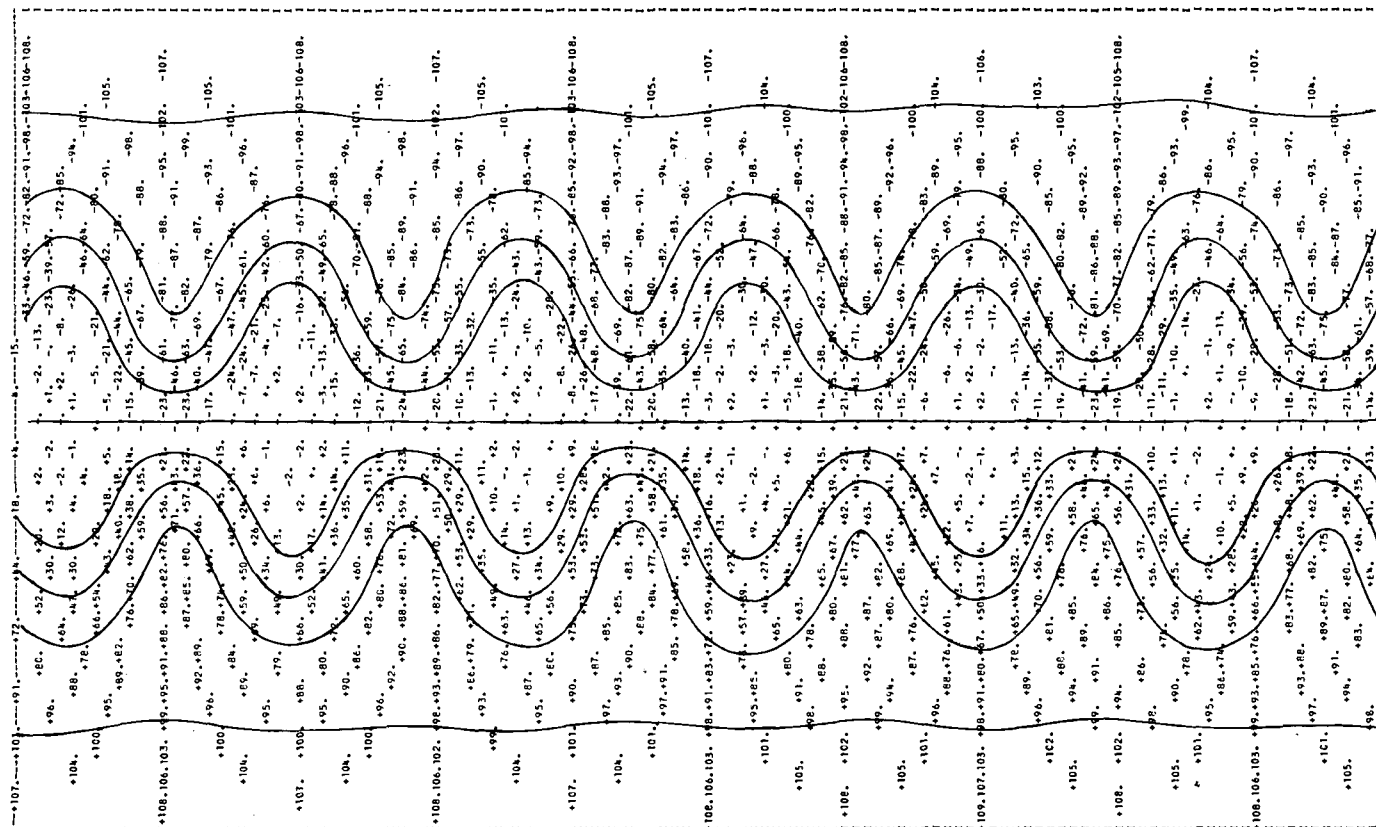


FIGURE 7.—Streamfunction after 8 days.

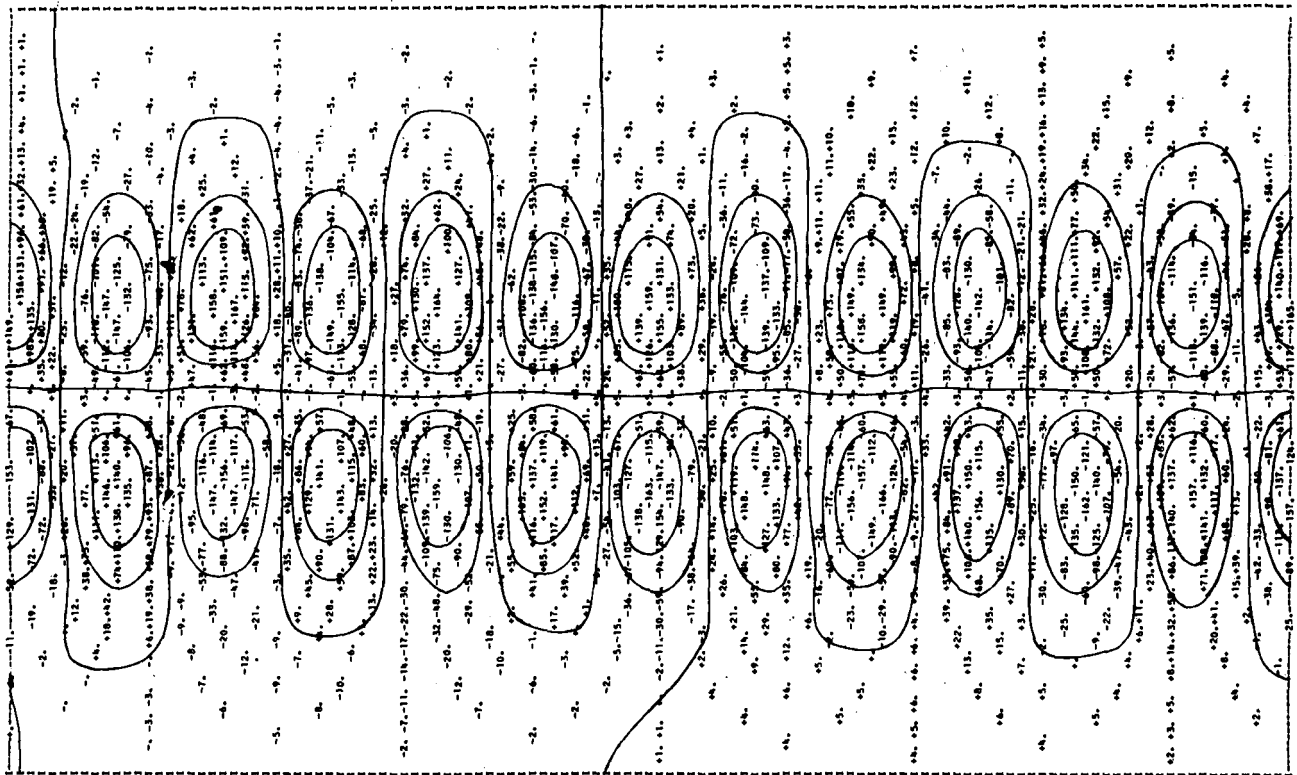


FIGURE 8.—Errors on the streamfunction after 8 days.

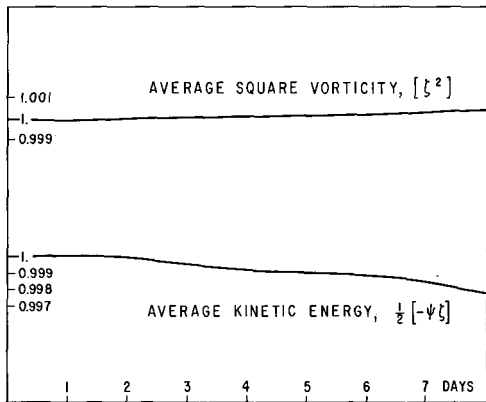


FIGURE 9.—Average square vorticity and average kinetic energy (relative to initial values), as a function of time.

agonal grid, gives a satisfactory approximation to the analytic solution for the chosen initial condition. Moreover, the scheme is nonlinearly stable, for any condition, because of its constraints on the quadratic quantities of kinetic energy and square vorticity.

The future importance of the icosahedral-hexagonal grid lies in its extension to the primitive equations for the large-scale motions of the atmosphere. The principal contributor to this investigation, R. Sadourny, is now developing such a scheme.

ACKNOWLEDGMENTS

This investigation was begun when R. Sadourny was a visitor at the University of California, Los Angeles, in 1965-66. It was completed by him after his return to the University of Paris.

For his interest in this study, and his support of R. Sadourny, we thank Professor Pierre Morel of the University of Paris. The authors also thank the computing facility of the University of California, Los Angeles, and the computing facility of the Centre National d'Études Spatiales, Brétigny, for making computing time available.

The investigation was supported, in part, by the Atmospheric Sciences Section, National Science Foundation, NSF Grants GP4190 and GA778.

REFERENCES

1. W. L. Gates and C. A. Riegel, "A study of Numerical Errors in the Integration of Barotropic Flow on a Spherical Grid," *Journal of Geophysical Research*, vol. 67, No. 2, Feb. 1962, pp. 773-784.
2. Y. Kurihara, "Numerical Integration of the Primitive Equations on a Spherical Grid," *Monthly Weather Review*, vol. 93, No. 7, July 1965, pp. 399-415.
3. E. H. Vestine, W. L. Sibley, J. W. Kern, and J. L. Carlstedt, "Integral and Spherical-Harmonic Analyses of the Geomagnetic Field for 1955.0, Part 2," *Journal of Geomagnetism and Geoelectricity*, vol. 15, No. 2, Aug. 1963, pp. 73-89.
4. A. Arakawa, "Computational Design for Long-Term Numerical Integration of the Equations of Fluid Motion: Two-Dimensional Incompressible Flow, Part I," *Journal of Computational Physics*, vol. 1, No. 1, July 1966, pp. 119-143.
5. S. M. Neamtan, "The Motion of Harmonic Waves in the Atmosphere," *Journal of Meteorology*, vol. 3, No. 2, June 1946, pp. 43-56.
6. D. K. Lilly, "On the Computational Stability of Numerical Solutions of Time-Dependent Non-Linear Geophysical Fluid Dynamics Problems," *Monthly Weather Review*, vol. 93, No. 1, Jan. 1965, pp. 11-26.

[Received December 18, 1967; revised February 9, 1968]